# Threshold Moving for Online Class Imbalance Learning with Dynamic Evolutionary Cost Vector

**Anonymous authors**
**Paper under double-blind review**

## Abstract

Existing online class imbalance learning methods fail to achieve optimal performance because their assumptions about enhancing minority classes are hardcoded in model parameters. To learn the model for the performance measure directly instead of using heuristics, we introduce a novel framework based on a dynamic evolutionary algorithm called Online Evolutionary Cost Vector (OECV). By bringing the threshold moving method from the cost-sensitive learning paradigm and viewing the cost vector as a hyperparameter, our method transforms the online class imbalance issue into a bi-level optimization problem. The first layer utilizes a base online classifier for rough prediction, and the second layer refines the prediction using a threshold moving cost vector learned via a dynamic evolutionary algorithm (EA). OECV benefits from both the efficiency of online learning methods and the high performance of EA, as demonstrated in empirical studies against four state-of-the-art methods on 30 datasets. Additionally, we show the effectiveness of the EA component in the ablation study by comparing OECV to its two variants, OECV-n and OECV-ea, respectively. This work reveals the superiority of incorporating EA into online imbalance classification tasks, while its potential extends beyond the scope of the class imbalance setting and warrants future research attention. We release our code[1] for future research.

## 1 Introduction

Online learning from streaming data is common in real-world applications, facing more challenges than offline learning due to limited time and memory resources. Online class imbalance learning involves scenarios where minority classes have notably fewer samples than the majority classes, which can detrimentally affect predictive performance, particularly for minority classes. Current efforts fall into three categories: data-level, algorithm-level, and ensemble approaches. Data-level methods use oversampling and undersampling to rebalance the datasets. Ensemble methods commonly work together with data-level algorithms by randomly resampling incoming data points for each base learner. Algorithm-level approaches react differently to samples from different classes, addressing the tendency to neglect the minority classes.

While designed differently, the three types of methodology all focus on how to efficiently utilize class imbalance information (e.g., imbalance ratio and data distribution) to handle the imbalance issue. However, to our knowledge, they all rely on assumptions about the expected enhancement level for minority classes, which are *ad hoc* and hardcoded in model parameters. For instance, cost-sensitive algorithms, one kind of algorithm-level approach, assign different costs for misclassifying classes based on the class size or performance. But determining optimal costs remains challenging (Liu & Zhou, 2010). In this article, we aim to explore how to achieve optimality concerning any given online performance metric directly without making *ad hoc* assumptions. It can extend beyond the scope of class imbalance, but we only focus on this online class imbalance setting in this work for simplicity. Due to the non-differentiability of many performance metrics, gradient-based optimization methods become impractical. Therefore, we focus on gradient-free optimization methods, particularly the family of evolutionary algorithms (EAs). EAs have been widely studied for classification tasks such as genetic programming (Espejo et al., 2009), learning classifier systems

[1] https://anonymous.4open.science/r/OECV-1088/

(Sigaud & Wilson, 2007), and evolution of neural networks (Rocha et al., 2007). Besides, recent studies have attempted to leverage EA to assist conventional algorithms in offline class imbalance learning problems (Pei et al., 2023). However, applying EAs to online class imbalance learning remains unexplored and challenging due to time and space constraints in streaming learning. More specifically, evolving classifiers on a large scale and accessing the entire dataset are impossible. Besides, the dynamic environment of concept drift may exist compared to offline learning. To this end, we have to examine a fundamental question: How can we create an online learner that combines two essential traits? That is, it should update fast under a dynamic environment like existing online models while also learning efficiently with non-differentiable objectives similar to EAs.

We propose a novel framework named Online Evolutionary Cost Vector (OECV) to answer this question. OECV is conceptualized as a bi-level optimization problem, with a probabilistic online classifier in the lower layer and a lightweight cost vector in the upper layer. The classifier extracts useful information from data to provide a rough prediction while the cost vector refines the decision boundary. In the case of concept drift, especially the prior drift where class size changes, a dynamic evolutionary algorithm is applied to track optimal cost vectors using recent samples contained in a fixed-size buffer. The most crucial difference between our dynamic EA and traditional EA is that it can track the optimal cost vector in a non-stationary environment by maintaining population diversity instead of converging. Our approach can learn with non-differentiable objectives under dynamic environments using a dynamic EA-based cost vector decision head and update in a few computation efforts since the cost vector is lightweight.

The motivation for formulating OECV as a bi-level architecture is highly inspired by the threshold moving method (Kukar et al., 1998; Zhou & Liu, 2005; Sheng & Ling, 2006; Voigt et al., 2014; Hancock et al., 2022) from the paradigm of cost-sensitive learning. The gist of the threshold moving is weighting the probabilistic prediction by the cost vector, which contains the relative cost of misclassifying each class. While the cost vector used in our method is essentially the same as that in the threshold moving method, however, the cost vector is usually predefined in the context of cost-sensitive learning. The key point in understanding our motivation is viewing the cost vector as a set of hyperparameters. This would interpret OECV as an online hyperparameter optimization (HPO) method built upon the threshold moving method. The simplest way of setting the hyperparameter in class imbalance learning is to set it inversely proportional to the class size, but it is not guaranteed to be an optimal solution. OECV, on the other hand, tries to optimize the "hyperparameter" using dynamic evolutionary algorithms on the fly. In viewing OECV as a kind of HPO, its two levels correspond to searching parameters and hyperparameters separately, where parameters (base classifier) give an rough prediction and hyperparameters (cost vector) refine the prediction. This effectively unifies EAs and online class imbalance learning within a cohesive framework.

The main contributions of this paper are listed as follows:

1. This study is the first to explore the problem of online class imbalance learning using an EA approach. The novel approach OECV unifies EA and online class imbalance learning within a bi-level optimization framework by applying a cost vector, effectively addressing the performance-resource trade-off.

2. We present a novel dynamic evolutionary algorithm to learn the cost vector under potential concept drift adaptively and incorporate specific prior knowledge about class imbalance to guide the evolutionary learning simultaneously.

3. We study the superiority and efficiency of OECV across 30 real-world datasets. Empirical results show its ability to significantly outperform state-of-the-art (SOTA) methods and confirm the effectiveness of the EA component.

The remainder of this article is organized as follows. Section 2 presents related work. Section 3 details our proposed method. Experimental setup and results are discussed in Section 4. The paper is concluded in Section 5.

## 2 Related Work

Our article is related to online class imbalance learning, threshold moving methods, and evolutionary algorithm approaches for addressing the class imbalance.

### 2.1 Online Class Imbalance Learning

Approaches to address online class imbalance problems can typically be classified into three categories, as mentioned in the introduction: data-level, algorithm-level, and ensemble-based methods.

#### 2.1.1 Data-level Methods

Sampling methods work by oversampling and/or undersampling to rebalance data. An oversampling technique based on classification contribution degree is proposed in Jiang et al. (2021), generating synthetic samples by combining inter-class and intra-class information. SMOTE (Chawla et al., 2002) is a synthetic minority over-sampling technique used to balance the class distribution by generating new instances of the minority class. In online learning, it has been adopted in Online SMOTE (Wang & Pineau, 2016), which oversamples using training samples within a sliding window. C-SMOTE (Bernardo et al., 2020) addresses binary class imbalance by actively detecting concept drift via ADWIN (Bifet & Gavalda, 2007), a change detector with a sliding detection window, and applying SMOTE to the minority class in the sliding window. SRE (Ren et al., 2019) introduces a selection-based resampling mechanism to handle complex data distributions by considering recent sample properties. These methods heavily rely on *ad hoc* heuristics and hyperparameters, like safety degree (Jiang et al., 2021), sampling rate (Wang & Pineau, 2016), borderline factor, and disjunct factor (Ren et al., 2019), which potentially hinder optimal performance.

#### 2.1.2 Algorithm-level Methods

Qin et al. (2021) employs active learning to select the most important samples to train the classifier. Online one-class Support Vector Machines (Klikowski & Woźniak, 2020) is a kind of one-class classifier that creates a model for each class and achieves a one-class decomposition of multi-class problems. Algorithm-level approaches work by modifying the training process. Cost-sensitive learning methods are a type of popular algorithm in this approach. It assigns varying costs for misclassifying classes belonging to different classes to reduce the dominating influence of majority classes, and it is commonly assumed that minority classes incur higher costs. Our method belongs to this category. Ksieniewicz (2021) introduces Prior Imbalance Compensation (PIC) for batch learning of imbalanced data streams, which adjusts the decision made by the classifier using class prior probability to compensate for the minority classes. Yan et al. (2017) trains multiple classifiers with various cost matrices and make predictions by adaptive ensembling. However, it is confined to binary class cases and challenging to extend to multi-class scenarios due to the exponential growth in the number of candidate cost matrices. Other related works (Wang et al., 2021; Ding et al., 2018; Qin et al., 2021) in cost-sensitive methods are based on weighted extreme learning machine (WELM) (Zong et al., 2013), which is a super efficient single hidden layer neural network with a weighting strategy for class imbalance. WOS-ELM (Wang et al., 2021) integrates a weighting strategy akin to WELM with an online sequential extreme learning machine (Huang et al., 2005) (OSELM). WOS-ELMK (Ding et al., 2018) incorporates kernel mapping, addressing the non-optimal hidden node issue present in WOS-ELM. AI-WSELM (Qin et al., 2021) integrates active learning to significantly reduce labeling costs, demonstrating satisfactory performance compared to existing WELM variants. Despite their promising performance, the weight strategies within this family are explicitly tailored for ELM, limiting their generalizability to other online learning models. We notice that the class sizes are frequently utilized to determine weight strategy in literature. However, this approach does not ensure an optimal weighting schedule.

#### 2.1.3 Ensemble Methods

Ensemble methods, such as MOOB, MUOB (Wang et al., 2016), KUE (Cano & Krawczyk, 2020), ROSE (Cano & Krawczyk, 2022), and BEDCOE (LI et al., 2023), effectively tackle the problem by combining resampling techniques. MOOB and MUOB leverage time-decay class size to determine training times. Specifically, the

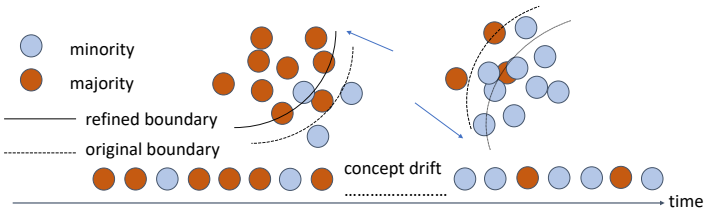


Figure 1: Illustration of the working mechanism of cost vector. The cost vector pushes the decision boundary towards the majority, and the dynamic evolutionary algorithm ensures the adaptability of the cost vector for potential concept drift.

training time for each base classifier is determined by sampling from a Poisson distribution, whose parameter is set according to the class size. The diversity is maintained by random training times on a sample for each base classifier. Kappa Updated Ensemble (KUE) combines online and block-based ensemble approaches and uses Kappa statistics to determine dynamic weighting and select base classifiers. After that, Cano & Krawczyk (2022) proposes an advanced method called ROSE to improve the robustness of KUE by employing adaptive self-tuning, adjusting its parameters, and ensembling the line-up dynamically. To directly deal with class imbalance, ROSE computes the imbalance ratio of each class based on recent samples to derive the training times of each sample. BEDCOE considers potential complex data distribution compared to other works and introduces a borderline enhanced strategy and a disjunct cluster-based oversampling for synthetic sample generation. Despite the improved performance achieved by using multiple base classifiers, the ensemble methods entail a trade-off between the diversity of the ensemble and training time.

### 2.2 Threshold Moving Method

The threshold moving method (Kukar et al., 1998; Zhou & Liu, 2005; Sheng & Ling, 2006; Voigt et al., 2014; Hancock et al., 2022) is a common technique in cost-sensitive learning. It trains a classifier on the original dataset and prioritizes classes with higher misclassification costs during prediction, using a predefined cost matrix. Formally, denote the cost matrix as $M_{ij}$, where $1 \leq i, j \leq C$, to represent the cost of misclassifying class $i$ to class $j$. Here $C$ is the number of classes. Let $O_i$, where $1 \leq i \leq C$, represent the probabilistic output with $\sum_{i=1}^{C} O_i = 1$ and $0 \leq O_i \leq 1$. The prediction is $\arg\max_i O'_i$ in the threshold moving method comparing to $\arg\max_i O_i$ in standard classifiers, where $O'_i$ is calculated according to

$$O'_i = \eta \sum_{j=1}^{C} O_i M_{ij} = \eta(\sum_{j=1}^{C} M_{ij}) O_i = \eta v_i O_i \tag{1}$$

Here $\eta$ is a normalization term such that $\sum_{i=1}^{C} O'_i = 1$ and $0 \leq O'_i \leq 1$. Note we can use the cost vector $v_i = \sum_{j=1}^{C} M_{ij}$ $(1 \leq i \leq C)$ of lower complexity $\mathcal{O}(C)$ instead. The cost vector represents the misclassification cost of class $i$ and adjusts the decision boundary toward less costly classes, making it harder to misclassify samples with higher costs. In this paper, the threshold moving method is adapted to online class imbalance learning by enabling the cost matrix/vector to be learnable in two novel ways, namely OECV-n and OECV, so that it can respond to the current stream behavior (Fig. 1) rather than being predefined. The baseline OECV-n is designed with time-decay class size, while the main algorithm OECV finds the optimal cost vector based on OECV-n and EA.

### 2.3 Evolutionary Algorithm for Class Imbalance Learning

Recent studies (Pei et al., 2023) have shown the potential of EA in addressing class imbalance, while most of the existing literature remains confined to offline scenarios. In Perry et al. (2015), a genetic algorithm (GA) is used to optimize a class-dependent cost matrix for the weighted updating of a classifier. Sun et al. (2006) introduces a cost-sensitive boosting algorithm that employs GA to optimize a class-dependent cost vector. ECSB (Lemnaru & Potolea, 2017) uses GA to optimize a class-dependent cost matrix and classifier

parameters simultaneously. GA is also applied to identify an optimal subset of instances in the majority class (Drown et al., 2009; Khoshgoftaar et al., 2010). In a cost-sensitive SVM method proposed in Cao et al. (2013), the misclassification cost ratio is optimized using particle swarm optimization. Furthermore, differential evolution (DE) has also been tried to optimize class-dependent cost matrices for cost-sensitive deep belief networks (Zhang et al., 2018; 2016). EA is also utilized to support data-level methods. For instance, Jiang et al. (2016) introduces GASMOTE, a GA-based SMOTE approach that optimizes sampling rates for minority class instances.

There are significant challenges to adapting these methods to online settings. Unlike offline learning, which receives all training data upfront, online learning lacks this comprehensive data overview. Besides, the model must continuously and rapidly adapt to potential concept drift rather than converging. To our knowledge, only Wang & Wang (2023) has adopted a similar idea of EA in online class imbalance learning. It picks base classifiers of different parameter configurations with the highest performance so far. However, characteristics of class imbalance in Wang & Wang (2023) are only used by the original resampling method, and the class imbalance issue is not handled by EA directly. Besides, it is currently tailored for binary classification tasks, making it unsuitable for multi-class scenarios.

## 3 Online Evolutionary Cost Vector (OECV)

In this section, we introduce *Online Evolutionary Cost Vector* (OECV) to illustrate the EA-based cost vector learning approach. Section 3.1 outlines the overall training process. Section 3.2 reformulates the problem into a bi-level optimization. Section 3.3 gives the baseline algorithm OECV-n, and Section 3.4 gives the EA-based algorithm OECV.

### 3.1 Overall Test-then-train Process of OECV

In a data stream $\{(X_t, y_t)\}_{t=1}^{+\infty}$, $X_t \in \mathbb{R}^d$ represents data and $y_t \in \{1, \ldots, C\}$ represents the class label. $C$ is the total number of classes. Uneven class prior distribution leads to class imbalance, and concept drift necessitates the algorithm to adapt to ever-changing data distribution. $X_t$ arrives strictly one by one, being predicted firstly by the latest classifier $\mathcal{H}_{t-1}^C$, and then refined using the cost vector $\mathbf{v}^*$ to give the final prediction $\mathbf{p}_t^*$. $\mathbf{p}_t^*$ is used together with true label $y_t$ that comes before $t+1$ to update classifier $\mathcal{H}_{t-1}^C$ to $\mathcal{H}_t^C$. This process is known as the "test-then-train" process.

We present OECV in Alg. 1. At the beginning of the data stream, the cost vector population $\mathcal{V}$ initializes randomly. At time step $t$, the model $\{\mathcal{H}_{t-1}^C, \mathbf{v}^*\}$, where $\mathcal{H}_t^C$ represents the latest online classifier, and $\mathbf{v}^*$ denotes the optimal cost vector discovered by EA up to time $t-1$, undergoes initial testing as depicted in Lines 1-2. Here, the online classifier offers an initial prediction, which is then refined by the cost vector. The classifier $\mathcal{H}^C$ updates by its own rule in Line 3. The class size $\Omega_{t-1}$ and fixed-size buffer $\mathcal{B}$ are updated in Lines 4-5, respectively. Cost vector population $\mathcal{V}$ evolves within the `if` statement (Lines 6-7) to yield a new population along with an optimal cost vector $\mathcal{V}^*$. We detail OECV in subsequent subsections individually.

### 3.2 Bi-level Optimization

Due to the impracticality of a full evolution, our framework only evolves partially, and breaks down both the model and the problem into two layers (See Fig. 2). The first layer, being an online classifier, offers a rough probabilistic prediction and updates by its own rule. The second layer, being a cost vector, refines the rough prediction and undergoes a dynamic optimization process via dynamic EA. As shown in the left part of Fig. 2, we denote the first and second layers as $\mathcal{H}_{1,t}$ and $\mathcal{H}_{2,t}$, respectively. The complete model is denoted by $\mathcal{H}_t = \{\mathcal{H}_{1,t}, \mathcal{H}_{2,t}\}$. The lower-level problem is to minimize a loss function $\ell_1(\mathcal{H}_1; X_t, y_t)$, which assesses the probabilistic prediction loss computed for each sample in the stream. The upper-level problem involves minimizing a non-differentiable performance metric $\ell_2(\mathcal{H}_{2,t}; p(\cdot; \mathcal{H}_{1,t}^*), y_t)$, which measures the refined prediction error based on the solution $\mathcal{H}_{1,t}^*$ of the first layer. The learning process of the upper layer occurs at a fixed frequency $f$ for computational efficiency. Importantly, the lower layer updates solely based on its own rule, and optimizing the upper layer does not affect the lower layer. The overall bi-level optimization problem is stated as $\min_{\mathcal{H}_{2,t}} \min_{\mathcal{H}_{1,t}} \ell_2(\mathcal{H}_{2,t}; p(\cdot; \mathcal{H}_{1,t}), y_t)$.

**Algorithm 1:** Training Procedures of Proposed OECV

**Input:** Classifier $\mathcal{H}^C_{t-1}$, class size $\Omega_{t-1}$, training sample $(X_t, y_t)$, evolutionary frequency $f$, optimal cost vector $\mathbf{v}^*$, cost vector population $\mathcal{V}$, buffer $\mathcal{B}$

**Output:** Prediction $\hat{y}_t$

Generate rough probabilistic prediction $\mathbf{p}_t$ using $\mathcal{H}^C_{t-1}$.
Produce refined prediction $\mathbf{p}^*_t$ as final prediction $\hat{y}_t$ using $\mathbf{p}_t$ and $\mathbf{v}^*$ by Eqn. 1.
Update $\mathcal{H}^C_{t-1}$ to $\mathcal{H}^C_t$ by its own rule.
Update class size $\Omega_{t-1} \to \Omega_t$ according to Eqn. 2.
Add the sample $(X_t, y_t)$ to $\mathcal{B}$.
**if** $t \mod f == 0$ **then**
    Evolve $\mathcal{V}$ by Alg. 2 with $\Omega_t$, $\mathcal{B}$ and $\mathcal{H}^C_t$, and update $\mathcal{V}$ and $\mathbf{v}^*$ based on evolution result.
**return** $\hat{y}_t$

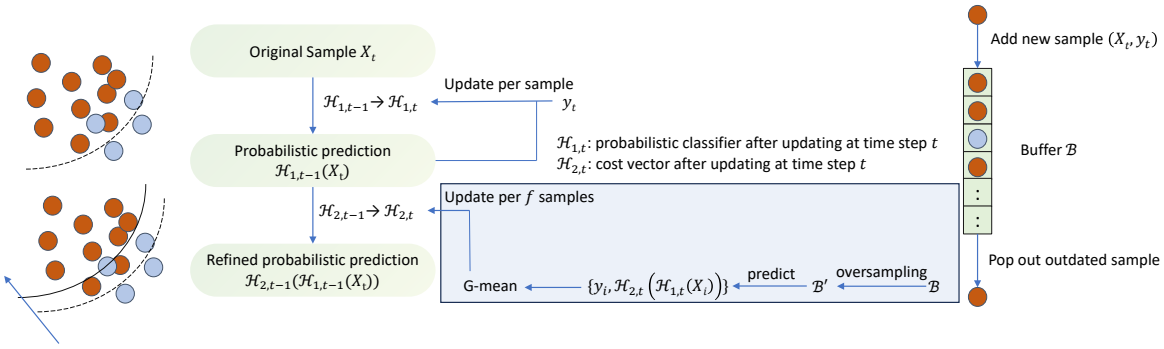


Figure 2: Illustration of OECV as a bi-level optimization problem (Section 3.2). The first layer consists of a probabilistic classifier, while the second layer is a cost vector (Section 2.2). A fixed-size buffer is maintained to perform oversampling and avoid potential overfitting. The cost vector is learned by a dynamic evolutionary algorithm at frequency $f$ on the oversampled buffer, using G-mean for objective evaluation (Section 3.4).

In this study, $\mathcal{H}_1$ is set to an online classifier $\mathcal{H}^C$ along with its $\ell_1$ from existing work. $\mathcal{H}^C$ may not consider the specific characteristics of the performance metric to be optimized. For instance, it may not care about the class imbalance in online class imbalance learning. $\mathcal{H}_2$ is set to a cost vector $\mathbf{v}$, and the choice of $\ell_2$ varies depending on specific needs, such as G-mean or balanced accuracy. In this way, only the upper layer is metric-specific. In the following subsections, we only focus on the learning strategies for the cost vector.

### 3.3 Learning Cost Vector with Time Decay Class Sizes

The first approach OECV-n(naive) employs time-decay class sizes (Wang et al., 2018) $\Omega_t = \{\omega_{i,t}\}_{i=1}^C$ at time $t$ to continuously track the imbalance status over time using a predefined time decay factor $\lambda$:

$$\omega_{k,t} = \lambda\omega_{k,t-1} + (1-\lambda)\cdot\mathbb{I}(y_t = k) \qquad 0 \le \lambda \le 1 \tag{2}$$

where $\omega_{k,t}$ represents the size of the $k$-th class at time step $t$, and $\mathbb{I}$ is the indicator function. Cost matrix $M_{ij}$ and cost vector $v_i$ are then determined heuristically as follows:

$$M_{ij} = \frac{\omega_{j,t}}{\omega_{i,t}} \qquad v_i = \sum_{j=1}^{C} M_{ij} \tag{3}$$

In other words, the model faces heavier penalties for misclassifying class $i$ to class $j$ as class $j$ gets larger or class $i$ gets smaller. It can adapt to current stream behavior by passively changing the imbalance status. However, it cannot guarantee optimal performance as it relies on the heuristic form of the cost matrix as well as the hyperparameter $\lambda$. The detailed training procedure of OECV-n is similar to that of OECV, by just removing all the use of evolution and replacing $\mathbf{v}^*$ in Alg. 1 by the cost vector determined by Eqn. 3

### 3.4 Learning Cost Vector with Dynamic Evolutionary Algorithm

**Algorithm 2:** Cost Vector Evolution

**Input:** Buffer $\mathcal{B}$, cost vector population $\mathcal{V}$, online classifier $\mathcal{H}^C$, number of neighbors $k$, sampling rate $r$, size of prior population $m$

**Output:** Optimal cost vector $\mathbf{v}^*$, cost vector population $\mathcal{V}$

1 // Maintain population diversity and integrate prior knowledge
2 Generate human-designed cost vector $\mathbf{v}_h$ using $\Omega_t$ by Eqn. 3.
3 Create prior population $\{\mathbf{v}^{(i)}\}_{i=1}^{m}$ based on $\mathbf{v}_h$ using Eqn. 4, and add to $\mathcal{V}$.
4 // Oversampling for data diversity
5 Initialize augmented buffer $\mathcal{B}'$ with samples from $\mathcal{B}$.
6 **for** $X_t$ *in* $\mathcal{B}$ **do**
7  **for** $r-1$ *times* **do**
8  Find $k$ nearest neighbors of $X_t$ and randomly select $X_t'$ from them.
9  Generate a new sample using Eqn. 5 with $\alpha \sim U(0,1)$, and add it to $\mathcal{B}'$.
10 // Evolution
11 Produce rough probabilistic prediction $\{\mathbf{p}_i\}_{i=1}^{|\mathcal{B}'|}$ for each sample in $\mathcal{B}'$ using $\mathcal{H}^C$.
12 For each $\mathbf{v}^{(k)}$, produce refined predictions $\{\mathbf{p}_i^{(k)}\}_{i=1}^{|\mathcal{B}'|}$ using $\{\mathbf{p}_i\}_{i=1}^{|\mathcal{B}'|}$ (Eqn. 1).
13 Calculate fitness $f^{(k)}$ for $\mathbf{v}^{(k)}$ based on $\{\mathbf{p}_i^{(k)}\}_{i=1}^{|\mathcal{B}'|}$ and true labels $\{y_i\}_{i=1}^{|\mathcal{B}'|}$.
14 Evolve $\mathcal{V}$ for one generation by crossover and mutation using $\{f^{(k)}\}_{k=1}^{|\mathcal{V}|}$. Calculate $\{f^{(k)}\}_{k=1}^{|\mathcal{V}|}$ to find the optimal solution $\mathbf{v}^*$ by comparing fitness.
15 **return** $\mathbf{v}^*$, $\mathcal{V}$

Compared to designing with time-decay class size, EAs can find cost vectors that optimize performance measures directly. The evolution process along two related tricks of the resulting OECV are illustrated as follows. See the complete algorithm in Alg. 2.

#### 3.4.1 Evolution

- **Chromosome Encoding**: The cost vector $\mathbf{v}^{(k)}$ is encoded into a chromosome straightforwardly, with the $C$-dimensional vector being the chromosome.
- **Fitness Calculation**: The chance of passing genetic information to subsequent generations relies on the fitness of a cost vector. We maintain recent samples in a fixed-size buffer $\mathcal{B}$ for fitness calculation[2]. $\mathcal{B}$ is enlarged into $\mathcal{B}'$ by oversampling (See next subsection) before being used for fitness evaluation. Specifically, we first do classification using the latest classifier $\mathcal{H}^C$ on $\mathcal{B}'$, resulting in the set of rough probabilistic predictions $\{\mathbf{p}_i\}_{i=1}^{|\mathcal{B}'|}$. For each individual $\mathbf{v}^{(k)}$, it refines the rough predictions to give a set of final predictions $\{\mathbf{p}_i^{(k)}\}_{i=1}^{|\mathcal{B}'|}$. $\{\mathbf{p}_i^{(k)}\}_{i=1}^{|\mathcal{B}'|}$ along with the set of true labels $\{y_i\}_{i=1}^{|\mathcal{B}'|}$ are then used to calculate a performance metric as the fitness $f^{(k)}$ of $\mathbf{v}^{(k)}$. With the set of fitness $\{f^{(k)}\}_{k=1}^{|\mathcal{V}|}$, the optimal individual (cost vector) can be determined straightforwardly. Note the performance metric used here is the corresponding offline metric (e.g., G-mean) instead of the online metric (e.g., online G-mean) so that the fitness calculation is not affected by the order of samples in $\mathcal{B}'$.
- **Genetic Operator**: EA employs genetic operators to produce new cost vectors by crossover and mutation based on the fitness value of individuals. Any single objective genetic operator may be used in the current framework.

If the generation of new cost vectors at Line 15 in Alg. 2 is removed, while the selection of the optimal individual in Line 16 is retained, we get a comparison algorithm OECV-ea as demonstrated in the ablation

[2]If additional memory is unavailable, an adaptive generative model can be used to generate samples in replace of the buffer. But it is not the focus of this work.

study. In this case, OECV-ea can be used to show whether OECV works by finding better individuals with evolution instead of simply relying on the extra data in the buffer to select a good solution from a large number of candidates.

#### 3.4.2 Maintain Population Diversity and Integrate Prior Knowledge

The cost vector designed by time-decay class size as in OECV-n can be used to guide EA. This benefits OECV by integrating the prior knowledge of imbalance status and preventing it from converging to a temporary optimal solution. Analogous to the time decay class size approach in spirits, the dynamic evolutionary also acts passively to counter the effect of concept drift, i.e., it would not detect the concept drift directly. We want to emphasize that this approach may not be the best choice in more complicated scenarios since it currently only focuses on the class-prior concept drift. How to adapt to more complicated drift scenarios is beyond the scope of this work. Specifically, we add $m$ different cost vectors $\{\mathbf{v}^{(i)}\}_{i=1}^{m}$ randomly generated by $\mathbf{v}_h$ from Eqn. 3 in a heuristic way:

$$\mathbf{v}^{(i)} = \mathbf{v}_h + \mathbf{w} \qquad w_j \sim U_j\left(0, \frac{i}{m}\right) \tag{4}$$

Recall in the definition of cost vector (Eqn. 1), we require each dimension of $\mathbf{v}^{(i)} = 1$ be in $[0, 1]$ and sum up to 1. Therefore, each dimension of $\mathbf{v}^{(i)}$ is clipped to $[0, 1]$ and re-normalized. $\{\mathbf{v}^{(i)}\}_{i=1}^{m}$ are then merged with the previous population to form the initial population for later evolution. After a fixed frequency $f$, the prior population is mixed in, and the population evolves over one generation.

#### 3.4.3 Oversampling for Data Diversity

To ensure accurate fitness calculation, an oversampling trick for enhancing data diversity is applied to $\mathcal{B}$. This creates an augmented buffer $\mathcal{B}'$. Specifically, we expand $\mathcal{B}$ to $r$ times its original size by generating $r-1$ samples $\{(X_t^{(i)}, y_t^{(i)})\}_{i=1}^{r-1}$ $(r \in \mathbb{N}_+)$ for each sample $(X_t, y_t)$:

$$X_t^{(i)} = X_t + \alpha \cdot (X_t' - X_t), \quad y_t^{(i)} = y_t \tag{5}$$

where $\alpha \sim U(0, 1)$ and $X_t'$ is randomly selected from $k$ nearest neighbors of $X_t$.

## 4 Experimental Studies

This section evaluates OECV from four aspects: comparing it to SOTA methods, testing the effectiveness of EA, evaluating runtime efficiency, and exploring its inner workings mechanism.

### 4.1 Experimental Setup

We use 30 datasets in total as shown in Table 1, including 10 streaming datasets (Elec, Abrupt, Gradual, Incremental1, Luxembourg, NOAA, Ozone, Airlines, Covtype, Incremental2, available in the USP-DS repository (Souza et al., 2020)) and 20 real-world offline datasets (remaining 20 datasets in Table 1, available in the Keel repository (Derrac et al., 2015)). The 20 offline datasets are processed in a streaming way to simulate online scenarios. The overall static imbalance ratio for each dataset illustrates the severity of class imbalance, while fluctuation of class imbalance ratio throughout the online learning scenario exists.

The initial 30% samples of each stream are used for model initialization in an offline fashion. The initialization samples are further split into two datasets in equivalent sizes for training the classifier and the cost vector separately. In this stage, the cost vector population evolves 10 generations to give an initial population for later online training. The buffer size $|\mathcal{B}|$ for OECV is fixed at 200 samples, and the oversampling rate is set to 3 for all datasets. Offline G-mean is used for fitness evaluation on the augmented buffer. The cost vector evolves every 5 sample (i.e., $f = 5$), with the number of individuals set to 25. We employ DE/best/1/L (Opara & Arabas, 2019) as the genetic operator. The implementation of evolutionary algorithms is easy and straightforward by directly adopting from the existing Python packages (such as geatpy [3], which was

[3] https://geatpy.github.io/

Table 1: Overview of the dataset. "#Data" denotes the total number of samples within this dataset, "#Fea" denotes the number of features, "#Class" denotes the number of classes, and IR denotes the overall static imbalance ratio being computed as the ratio between the largest and smallest class sizes.

| Dataset | #Data | #Fea | #Class | IR | Dataset | #Data | #Fea | #Class | IR | Dataset | #Data | #Fea | #Class | IR |
|---|---|---|---|---|---|---|---|---|---|---|---|---|---|---|
| Elec | 5000 | 8 | 2 | 1.6 | Abalone1 | 2338 | 8 | 2 | 39.3 | Win1 | 691 | 11 | 2 | 68.1 |
| Abrupt | 5000 | 33 | 6 | 4.0 | Abalone2 | 1622 | 8 | 2 | 49.7 | Win2 | 1599 | 11 | 2 | 29.2 |
| Gradual | 5000 | 33 | 6 | 171.2 | Car1 | 1728 | 6 | 2 | 24.0 | Win3 | 656 | 11 | 2 | 35.4 |
| Incremental1 | 5000 | 33 | 6 | 1.0 | Car2 | 1728 | 6 | 2 | 25.6 | Win4 | 1482 | 11 | 2 | 58.3 |
| Luxembourg | 1901 | 31 | 2 | 1.06 | Kddcup | 2225 | 41 | 2 | 100.1 | Win5 | 900 | 11 | 2 | 44.0 |
| NOAA | 5000 | 8 | 2 | 2.4 | Kr | 2901 | 6 | 2 | 26.6 | Yeast1 | 947 | 8 | 2 | 30.6 |
| Ozone | 2534 | 72 | 2 | 14.8 | Segment | 2308 | 19 | 2 | 6.0 | Yeast2 | 1484 | 8 | 10 | 92.6 |
| Airlines | 5000 | 7 | 2 | 2.1 | Shuttle1 | 3316 | 9 | 2 | 66.7 | Yeast3 | 1484 | 8 | 2 | 8.1 |
| Covtype | 5000 | 54 | 7 | 7.0 | Shuttle2 | 1829 | 9 | 2 | 13.9 | Yeast4 | 1484 | 8 | 2 | 32.7 |
| Incremental2 | 5000 | 33 | 6 | 25.4 | Thyroid | 720 | 21 | 3 | 39.2 | Yeast5 | 1484 | 8 | 2 | 41.4 |

used in our experiments). All the hyperparameters related to genetic operators are set to the default values. Specifically, the scaling factor of DE is set to 0.5, and exponential crossover is applied with the probability of crossover set to 0.7.

We compare OECV with four SOTA online multi-class imbalance learning methods: MOOB, MUOB (Wang et al., 2016), AI-WSELM (Qin et al., 2021), and BEDCOE (LI et al., 2023). The total number of base learners is set to 10, following (Wang et al., 2016; LI et al., 2023). All methods adhere to a strict online learning setup. Multilayer perceptron serves as the base classifier for all methods, except AI-WSELM, following the setup in Wang et al. (2016). Prequential G-mean with a fading factor of 0.99 is selected as performance metrics, following Wang et al. (2018) and LI et al. (2023). Mean performance across 10 runs is evaluated on the remaining samples after the initialization number. Friedman tests (Demšar, 2006) are used to compare competing methods across datasets statistically. The null hypothesis (H0) posits that all models are equivalent in terms of the predictive performance metric. The alternative hypothesis (H1) suggests that at least one pair of methods differs significantly. If H0 is rejected, the Conover test (Conover & Iman, 1979) is conducted as the post-hoc test.

### 4.2 Performance Comparison

We can see from Table 2(a) that in terms of G-mean, OECV performs the best in 14 out of 30 datasets and the 2nd best in 8 datasets. Friedman tests at significance level 0.05 reject H0 with $p$-value $1.11 \times 10^{-3}$, showing a significant difference between methods. Average ranks ("avgRank") across datasets are reported to show how well each method performs compared to others across datasets. The average rank of OECV is 1.967, being the best. Post-hoc tests are then conducted to detect whether OECV has a significant difference from the competitors, for which OECV is chosen as the control method. Post-hoc comparisons show that OECV can significantly outperform all of the competitors.

### 4.3 Ablation Study

Two comparison models OECV-n and OECV-eahave been built in Section 3.3 and Section 3.4, which differ from OECV by just the way on learning cost vector. They are employed here to study the effectiveness of EA. We would expect the performance of OECV, with the full assistance of evolutionary optimization, to be the best. The performance of OECV-ea should be in the middle since while evolution is not used, several candidates of cost vectors are still under consideration for selecting the best one using extra data. The performance of OECV-n should be the worst because only human knowledge is used. If this occurs, we can conclude that the EA used for optimizing the cost vector is crucial for dealing with class imbalance, and extra data in the buffer is not the determinative reason for performance improvement.

Table 2(b) shows the result in terms of G-mean. The three methods are compared to each other, with Wilcoxon signed rank tests (Wilcoxon, 1992) used to determine if there are significant differences between

Table 2: Performance comparison in terms of G-mean (%). Each entry is the mean±std performance across 10 runs. The best performance on each dataset is highlighted in bold, and the 2nd best performance is highlighted in italics. The last row lists the average ranks (avgRank) of each model across datasets in each subtable. Part (a) compares SOTA methods and the proposed OECV. A significant difference against OECV is highlighted in yellow. Part (b) reports the ablation results between variants of OECV.

(a) Performance comparison

| Dataset | AI-WSELM | MOOB | MUOB | BEDCOE | OECV |
|---|---|---|---|---|---|
| Elec | 78.2±1.6 | *90.9±0.2* | 88.7±0.4 | **95.5±0.1** | 83.7±0.9 |
| Abrupt | **66.2±1.4** | 60.2±1.7 | 60.4±2.2 | 60.0±0.4 | *62.8±0.6* |
| Gradual | 0.0±0.0 | *22.4±9.1* | 0.1±0.3 | **34.8±20.4** | 8.5±4.2 |
| Incremental1 | 46.0±0.7 | **53.8±0.6** | 48.5±2.0 | *52.9±0.4* | 46.4±1.5 |
| Luxembourg | 85.5±2.4 | **100.0±0.0** | **100.0±0.0** | **100.0±0.0** | **100.0±0.0** |
| NOAA | *71.3±0.8* | 65.3±0.7 | 64.6±0.6 | 68.2±0.7 | **73.1±0.5** |
| Ozone | 65.0±2.9 | 72.3±1.8 | **78.0±0.6** | 70.6±1.3 | *77.1±1.7* |
| Airlines | *50.8±1.0* | 34.6±2.8 | 47.6±1.6 | 50.6±0.4 | **51.8±0.9** |
| Covtype | 0.0±0.0 | **65.4±0.8** | 0.0±0.0 | *64.6±1.2* | 28.6±1.5 |
| Incremental2 | 0.8±0.2 | *30.8±5.0* | 0.9±1.2 | **40.9±1.6** | 15.6±1.6 |
| Abalone1 | 43.6±5.2 | 55.0±0.9 | *64.5±3.8* | 59.1±0.8 | **67.8±4.3** |
| Abalone2 | **48.0±9.3** | 4.6±0.0 | 26.8±8.2 | 33.2±0.0 | *38.7±7.6* |
| Car1 | **80.4±2.9** | 33.3±4.3 | 56.3±4.9 | 44.5±5.0 | *78.2±2.2* |
| Car2 | **96.5±2.9** | 74.9±0.7 | 79.8±3.7 | 74.4±1.5 | *96.1±1.0* |
| Kddcup | 78.1±11.8 | **100.0±0.0** | 95.9±3.5 | **100.0±0.0** | **100.0±0.0** |
| Kr | 94.3±1.7 | *94.4±0.7* | 90.5±1.8 | 90.2±0.7 | **94.7±1.3** |
| Segment | 98.7±0.4 | 98.9±0.1 | 93.0±0.6 | *99.0±0.0* | **99.1±0.1** |
| Shuttle1 | **100.0±0.0** | 99.4±0.6 | 97.9±1.7 | 99.0±0.9 | *99.9±0.0* |
| Shuttle2 | 99.4±0.1 | 99.6±0.0 | **99.8±0.1** | *99.7±0.1* | *99.7±0.0* |
| Thyroid | 29.0±14.0 | 38.9±2.7 | 0.6±0.0 | *56.7±2.2* | **71.6±1.5** |
| Win1 | 29.1±34.1 | 6.8±0.0 | 6.8±0.0 | *36.5±36.4* | **80.6±1.2** |
| Win2 | 39.0±4.8 | 15.4±5.1 | **62.0±5.0** | 27.3±1.4 | *59.2±3.6* |
| Win3 | 26.2±11.3 | 22.1±2.4 | 19.6±10.0 | *26.5±2.8* | **79.9±1.2** |
| Win4 | 9.7±10.7 | *43.2±11.6* | 16.7±9.5 | 27.7±1.6 | **50.6±5.7** |
| Win5 | 22.8±19.3 | *32.8±4.7* | 11.0±4.2 | 14.7±0.0 | **53.3±7.1** |
| Yeast1 | *47.8±8.0* | 32.0±0.5 | 36.1±13.8 | 33.2±4.1 | **48.0±18.9** |
| Yeast2 | **28.0±6.0** | 0.1±0.1 | 0.0±0.0 | *8.8±4.2* | 0.2±0.4 |
| Yeast3 | 81.5±2.3 | *89.2±0.3* | **89.8±1.2** | 87.5±0.3 | 87.8±1.0 |
| Yeast4 | 72.9±6.6 | **86.5±0.8** | *82.4±9.5* | 71.7±2.8 | 81.7±5.7 |
| Yeast5 | *70.3±3.8* | 64.1±1.9 | 51.7±7.1 | 53.1±3.0 | **86.5±1.7** |
| avgRank | 3.35 | 3.133 | 3.517 | 3.033 | 1.967 |

(b) Ablation studies

| OECV-n | OECV | OECV-ea |
|---|---|---|
| 83.1±0.4 | **83.7±0.9** | *83.6±0.9* |
| 62.0±0.7 | **62.8±0.6** | *62.6±0.9* |
| **15.8±2.5** | *8.5±4.2* | 4.3±2.8 |
| **46.4±1.5** | *46.2±1.2* | |
| **100.0±0.0** | **100.0±0.0** | **100.0±0.0** |
| *73.0±0.5* | **73.1±0.5** | 72.9±0.5 |
| 71.8±1.9 | **77.1±1.7** | *76.1±1.6* |
| 50.7±0.5 | **51.8±0.9** | *51.7±0.8* |
| **38.7±1.1** | *28.6±1.5* | 26.6±1.3 |
| **21.2±1.8** | *15.6±1.6* | 13.0±1.0 |
| 55.7±3.0 | **67.8±4.3** | *59.0±5.7* |
| 25.6±0.1 | **38.7±7.6** | *33.1±5.9* |
| 77.0±3.1 | **78.2±2.2** | *77.5±2.0* |
| 94.7±1.2 | **96.1±1.0** | *95.2±0.9* |
| **100.0±0.0** | **100.0±0.0** | **100.0±0.0** |
| 91.5±0.8 | **94.7±1.3** | *92.2±1.3* |
| *99.1±0.1* | *99.1±0.1* | **99.4±0.1** |
| **99.9±0.0** | **99.9±0.0** | **99.9±0.0** |
| **99.7±0.0** | **99.7±0.0** | 99.6±0.0 |
| 68.5±3.8 | *71.6±1.5* | **73.6±2.2** |
| 79.9±0.1 | **80.6±1.2** | **80.6±0.9** |
| 48.1±0.9 | **59.2±3.6** | *49.6±1.9* |
| 39.0±4.2 | **79.9±1.2** | *60.6±12.9* |
| 18.9±7.7 | **50.6±5.7** | *29.1±4.1* |
| **53.3±5.6** | **53.3±7.1** | 41.0±7.4 |
| *16.5±0.9* | **48.0±18.9** | 15.5±0.2 |
| *0.0±0.0* | **0.2±0.4** | *0.0±0.0* |
| 85.0±1.1 | **87.8±1.0** | *86.8±0.8* |
| 68.3±4.0 | **81.7±5.7** | *75.0±3.7* |
| *84.8±0.1* | **86.5±1.7** | 81.8±2.8 |
| 2.467 | 1.333 | 2.2 |

them. We can see that the average rank of OECV (1.333) is better than that of OECV-n (2.467) and OECV-ea (2.2). Wilcoxon signed rank test rejects H0 with $p$-value 0.0036 and $9.62 \times 10^{-5}$, respectively, meaning OECV is significantly superior to OECV-n and OECV-ea. But in comparison between OECV-ea and OECV-n, the average rank of OECV-ea (2.2) is better than OECV-n (2.467), and the Wilcoxon signed rank test fails to reject H0 with $p$-value 0.178, meaning there is no significant difference between OECV-ea and OECV-n. From the comparison between OECV and OECV-n, we see that eliminating the whole EA strategy would significantly decline performance. However, this can be caused by the extra data from the buffer used in OECV. We can see from the comparison between OECV-ea and OECV, as well as OECV-ea and OECV-n, that the extra data does not play a determinative role. To see this, OECV-ea also uses extra data in finding optimal cost vector with performance set to the objective of performance metric, but it does not perform significantly better than OECV-n and performs significantly worse than OECV. This means it is the EA instead of extra data making OECV outperform SOTA methods, showing the effectiveness of EA.

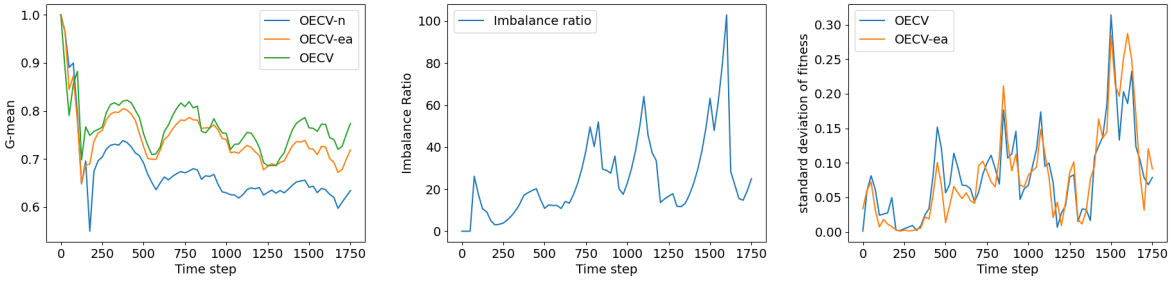


Figure 3: Prequential G-mean, imbalance ratio, and standard deviation of fitness of the population in dataset Ozone. The higher the standard deviation, the greater the diversity. Imbalance ratio is calculated by time-decay class sizes (Eqn. 2).

### 4.4 Further Discussions

We explore two related questions to assess the working mechanism of OECV.

#### 4.4.1 Analysis on Population Diversity

We explore whether OECV can maintain population diversity over time instead of converging. The population diversity enables OECV to track the optimal cost vector instead of converging to a certain solution. We present the standard derivation of individual fitness in Fig. 3 with a further analysis of the Spearman correlation (Fieller et al., 1957). The result shows correlation coefficients of 0.715 and 0.772 between the imbalance ratio and standard deviation (std) of fitness of OECV and OECV-ea, respectively, being strongly correlated. It also shows a high correlation coefficient of 0.869 between the std of fitness of OECV and OECV-ea. We can draw two observations: 1) The diversity adapts to data stream behavior. This means OECV and OECV-ea can expand the exploration of new cost vectors (high std) during a concept drift while adopting temporary elitists by leveraging learned knowledge about class imbalance (low std) during the steady stream. 2) Despite similar diversity and changing behavior, OECV outperforms OECV-ea. This indicates the superiority of EA in that it can maintain a population of cost vectors with higher quality under the same diversity.

#### 4.4.2 Analysis on EA-based Cost Vector

We explore how the cost vector found by the EA-based method outperforms that of OECV-n. We define the weight ratio (WR) as $\frac{v_1}{v_0}$ to visualize the cost vector in a binary classification scenario in Fig. 4. Here, $v_i$ represents the $i$-th dimension of the cost vector. Analogous to the imbalance ratio, the WR serves as a belief of the imbalance level indicated by the cost vector. We analyze the Spearman correlation between the WR of three variants and the imbalance ratio, yielding correlation coefficients of 0.971, 0.897, and 0.887 for OECV-n, OECV-ea, and OECV respectively, indicating strong correlations. This means the cost vectors found by EA can also reflect the beliefs about class imbalance, while some of these beliefs are sacrificed to seek more appropriate values of the cost vector in finding the optimal solution. Besides, Fig. 4 illustrates the challenge of finding the optimal solution by *ad hoc* assumptions: While OECV outperforms that of OECV-n, the WR of OECV fluctuates compared to OECV-n. This suggests that relying solely on the imbalance ratio is insufficient for identifying the best cost vector. The dynamic evolutionary algorithm addresses this limitation by directly setting the performance measure as the objective and avoiding heuristic reliance.

## 5 Conclusion

This article introduces a novel approach Online Evolutionary Cost Vector (OECV) along with its two variants to tackle the online class imbalance issue by eliminating heuristic assumptions about class imbalances widely used in existing methods. The OECV instead tries to maximize performance on any specified performance metrics directly. This is achieved by adopting a dynamic evolutionary algorithm for online model evolution.

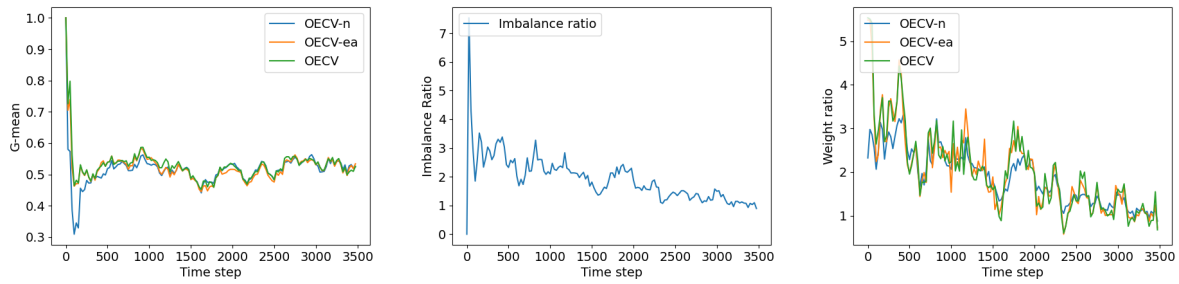


Figure 4: Prequential G-mean, imbalance ratio, and weight ratio in dataset Airlines. Imbalance ratio is calculated by time-decay class sizes (Eqn. 2).

The model is explicitly deconstructed into two layers: an online classifier for rough probabilistic prediction and a cost vector for refining the decision boundary. The cost vector is the only part subject to the dynamic evolutionary algorithm used for directly optimizing any specific performance metrics. This bi-level architecture is motivated by viewing the cost vector as a hyperparameter in the threshold moving method and the evolutionary algorithm as an approach to fine-tune the cost vector. This is based on the assumption that the cost vector, utilized to adjust the decision boundary, has an optimal value that yields the best online metric for a dynamic base classifier. A dynamic evolutionary algorithm is employed to find a superior value to a human-designed counterpart. Cost vectors designed by time-decay class size are integrated into the prior population to sustain population diversity and integrate prior knowledge. To mitigate overfitting, an oversampling method is used to augment the buffer and attain more beneficial evolutionary results. Comparison with SOTA methods, ablation studies, and runtime comparison demonstrate the validity and efficiency of our approach. Analysis of the working mechanism of OECV reveals how it can generate a superior cost vector compared to the human-designed counterpart.

We want to emphasize that the potential of the OECV framework extends beyond the class imbalance setting. It has further exploration values in various other classification tasks. High performance across a broad range of metrics unrelated to class imbalance can be achieved with only slight adjustments to the cost vector. For instance, OECV can simultaneously serve multi-objective purposes by optimizing for multiple metrics, including accuracy, recall, and F1-score.

## References

Alessio Bernardo, Heitor Murilo Gomes, Jacob Montiel, Bernhard Pfahringer, Albert Bifet, and Emanuele Della Valle. C-smote: Continuous synthetic minority oversampling for evolving data streams. In *2020 IEEE International Conference on Big Data (Big Data)*, pp. 483–492. IEEE, 2020.

Albert Bifet and Ricard Gavalda. Learning from time-changing data with adaptive windowing. In *Proceedings of the 2007 SIAM international conference on data mining*, pp. 443–448. SIAM, 2007.

Alberto Cano and Bartosz Krawczyk. Kappa updated ensemble for drifting data stream mining. *Machine Learning*, 109:175–218, 2020.

Alberto Cano and Bartosz Krawczyk. Rose: robust online self-adjusting ensemble for continual learning on imbalanced drifting data streams. *Machine Learning*, 111(7):2561–2599, 2022.

Peng Cao, Dazhe Zhao, and Osmar Zaiane. An optimized cost-sensitive svm for imbalanced data learning. In *Pacific-Asia conference on knowledge discovery and data mining*, pp. 280–292. Springer, 2013.

Nitesh V Chawla, Kevin W Bowyer, Lawrence O Hall, and W Philip Kegelmeyer. Smote: synthetic minority over-sampling technique. *Journal of artificial intelligence research*, 16:321–357, 2002.

William Jay Conover and Ronald L Iman. On multiple-comparisons procedures. *Los Alamos Sci. Lab. Tech. Rep. LA-7677-MS*, 1:14, 1979.

Janez Demšar. Statistical comparisons of classifiers over multiple data sets. *The Journal of Machine learning research*, 7:1–30, 2006.

J Derrac, S Garcia, L Sanchez, and F Herrera. Keel data-mining software tool: Data set repository, integration of algorithms and experimental analysis framework. *J. Mult. Valued Log. Soft Comput*, 17:255–287, 2015.

Shuya Ding, Bilal Mirza, Zhiping Lin, Jiuwen Cao, Xiaoping Lai, Tam V Nguyen, and Jose Sepulveda. Kernel based online learning for imbalance multiclass classification. *Neurocomputing*, 277:139–148, 2018.

Dennis J Drown, Taghi M Khoshgoftaar, and Naeem Seliya. Evolutionary sampling and software quality modeling of high-assurance systems. *IEEE Transactions on Systems, Man, and Cybernetics-Part A: Systems and Humans*, 39(5):1097–1107, 2009.

Pedro G Espejo, Sebastián Ventura, and Francisco Herrera. A survey on the application of genetic programming to classification. *IEEE Transactions on Systems, Man, and Cybernetics, Part C (Applications and Reviews)*, 40(2):121–144, 2009.

Edgar C Fieller, Herman O Hartley, and Egon S Pearson. Tests for rank correlation coefficients. i. *Biometrika*, 44(3/4):470–481, 1957.

John Hancock, Justin M Johnson, and Taghi M Khoshgoftaar. A comparative approach to threshold optimization for classifying imbalanced data. In *2022 IEEE 8th International Conference on Collaboration and Internet Computing (CIC)*, pp. 135–142. IEEE, 2022.

Guang-Bin Huang, Nan-Ying Liang, Hai-Jun Rong, Paramasivan Saratchandran, and Narasimhan Sundararajan. On-line sequential extreme learning machine. *Computational Intelligence*, 2005:232–237, 2005.

Kun Jiang, Jing Lu, and Kuiliang Xia. A novel algorithm for imbalance data classification based on genetic algorithm improved smote. *Arabian journal for science and engineering*, 41:3255–3266, 2016.

Zhenhao Jiang, Tingting Pan, Chao Zhang, and Jie Yang. A new oversampling method based on the classification contribution degree. *Symmetry*, 13(2):194, 2021.

Taghi M Khoshgoftaar, Naeem Seliya, and Dennis J Drown. Evolutionary data analysis for the class imbalance problem. *Intelligent Data Analysis*, 14(1):69–88, 2010.

Jakub Klikowski and Michał Woźniak. Employing one-class svm classifier ensemble for imbalanced data stream classification. In *Computational Science–ICCS 2020: 20th International Conference, Amsterdam, The Netherlands, June 3–5, 2020, Proceedings, Part IV 20*, pp. 117–127. Springer, 2020.

Paweł Ksieniewicz. The prior probability in the batch classification of imbalanced data streams. *Neurocomputing*, 452:309–316, 2021.

Matjaz Kukar, Igor Kononenko, et al. Cost-sensitive learning with neural networks. In *ECAI*, volume 15, pp. 88–94. Citeseer, 1998.

Camelia Lemnaru and Rodica Potolea. Evolutionary cost-sensitive balancing: A generic method for imbalanced classification problems. In *EVOLVE-A Bridge between Probability, Set Oriented Numerics, and Evolutionary Computation VI*, pp. 194–209. Springer, 2017.

Shuxian LI, Liyan SONG, Yiu-Ming CHEUNG, and Xin YAO. Bedcoe: Borderline enhanced disjunct cluster based oversampling ensemble for online multi-class imbalance learning. In *ECAI 2023: 26th European Conference on Artificial Intelligence, September 30–October 4, 2023, Kraków, Poland, Including 12th Conference on Prestigious Applications of Intelligent Systems (PAIS 2023): Proceedings*, pp. 1414–1421. IOS Press BV, 2023.

Xu-Ying Liu and Zhi-Hua Zhou. Learning with cost intervals. In *Proceedings of the 16th ACM SIGKDD international conference on Knowledge discovery and data mining*, pp. 403–412, 2010.

Karol R Opara and Jarosław Arabas. Differential evolution: A survey of theoretical analyses. *Swarm and evolutionary computation*, 44:546–558, 2019.

Wenbin Pei, Bing Xue, Mengjie Zhang, Lin Shang, Xin Yao, and Qiang Zhang. A survey on unbalanced classification: How can evolutionary computation help? *IEEE Transactions on Evolutionary Computation*, 2023.

Todd Perry, Mohamed Bader-El-Den, and Steven Cooper. Imbalanced classification using genetically optimized cost sensitive classifiers. In *2015 IEEE Congress on Evolutionary Computation (CEC)*, pp. 680–687. IEEE, 2015.

Jiongming Qin, Cong Wang, Qinhong Zou, Yubin Sun, and Bin Chen. Active learning with extreme learning machine for online imbalanced multiclass classification. *Knowledge-Based Systems*, 231:107385, 2021.

Siqi Ren, Wen Zhu, Bo Liao, Zeng Li, Peng Wang, Keqin Li, Min Chen, and Zejun Li. Selection-based resampling ensemble algorithm for nonstationary imbalanced stream data learning. *Knowledge-Based Systems*, 163:705–722, 2019.

Miguel Rocha, Paulo Cortez, and José Neves. Evolution of neural networks for classification and regression. *Neurocomputing*, 70(16-18):2809–2816, 2007.

Victor S Sheng and Charles X Ling. Thresholding for making classifiers cost-sensitive. In *Aaai*, volume 6, pp. 476–481, 2006.

Olivier Sigaud and Stewart W Wilson. Learning classifier systems: a survey. *Soft Computing*, 11:1065–1078, 2007.

Vinicius MA Souza, Denis M dos Reis, Andre G Maletzke, and Gustavo EAPA Batista. Challenges in benchmarking stream learning algorithms with real-world data. *Data Mining and Knowledge Discovery*, 34: 1805–1858, 2020.

Yanmin Sun, Mohamed S Kamel, and Yang Wang. Boosting for learning multiple classes with imbalanced class distribution. In *Sixth international conference on data mining (ICDM'06)*, pp. 592–602. IEEE, 2006.

Tobias Voigt, Roland Fried, Michael Backes, and Wolfgang Rhode. Threshold optimization for classification in imbalanced data in a problem of gamma-ray astronomy. *Advances in Data Analysis and Classification*, 8:195–216, 2014.

Boyu Wang and Joelle Pineau. Online bagging and boosting for imbalanced data streams. *IEEE Transactions on Knowledge and Data Engineering*, 28(12):3353–3366, 2016.

Liwen Wang, Yicheng Yan, and Wei Guo. Ensemble online weighted sequential extreme learning machine for class imbalanced data streams. In *2021 2nd International Symposium on Computer Engineering and Intelligent Communications (ISCEIC)*, pp. 81–86. IEEE, 2021.

Shuo Wang, Leandro L Minku, and Xin Yao. Dealing with multiple classes in online class imbalance learning. In *IJCAI*, pp. 2118–2124, 2016.

Shuo Wang, Leandro L Minku, and Xin Yao. A systematic study of online class imbalance learning with concept drift. *IEEE transactions on neural networks and learning systems*, 29(10):4802–4821, 2018.

Zhaoyang Wang and Shuo Wang. Online automated machine learning for class imbalanced data streams. In *2023 International Joint Conference on Neural Networks (IJCNN)*, pp. 1–8. IEEE, 2023.

Frank Wilcoxon. Individual comparisons by ranking methods. In *Breakthroughs in Statistics: Methodology and Distribution*, pp. 196–202. Springer, 1992.

Yan Yan, Tianbao Yang, Yi Yang, and Jianhui Chen. A framework of online learning with imbalanced streaming data. In *Proceedings of the AAAI Conference on Artificial Intelligence*, volume 31, 2017.

Chong Zhang, Kay Chen Tan, and Ruoxu Ren. Training cost-sensitive deep belief networks on imbalance data problems. In *2016 international joint conference on neural networks (IJCNN)*, pp. 4362–4367. IEEE, 2016.

Chong Zhang, Kay Chen Tan, Haizhou Li, and Geok Soon Hong. A cost-sensitive deep belief network for imbalanced classification. *IEEE transactions on neural networks and learning systems*, 30(1):109–122, 2018.

Zhi-Hua Zhou and Xu-Ying Liu. Training cost-sensitive neural networks with methods addressing the class imbalance problem. *IEEE Transactions on knowledge and data engineering*, 18(1):63–77, 2005.

Weiwei Zong, Guang-Bin Huang, and Yiqiang Chen. Weighted extreme learning machine for imbalance learning. *Neurocomputing*, 101:229–242, 2013.

# A Appendix

## A.1 Running Time Comparison

Since EA is known for high time complexity, we conduct a runtime experiment to show the practicality of OECV. All experiments are benchmarked on a server configured with Intel(R) Xeon(R) Gold 6338 CPU @ 2.00GHz. The geometric average of runtime across datasets is reported in the case of varying runtime scales across datasets. Specifically, suppose $N$ datasets are used, we report $\sqrt[N]{\prod_{i=1}^{N} t_i}$, where $t_i$ represents the runtime on the $i$-th dataset. Two key observations can be made from the results in Table 3. Firstly, while some methods exhibit significantly shorter runtimes, such as MUOB and OECV-n, this comes at the expense of their inferior performance, as evidenced in Table 2(a). Secondly, our approach demonstrates remarkable efficiency, as OECV achieves the best rank with tolerably short runtime compared to other SOTA methods. This validates the time efficiency and practicality of OECV despite using EA.

## A.2 Performance Comparison in Terms of Balanced Accuracy

In Table 4, we include a complementary performance comparison in terms of balanced accuracy of Section 4.2.

We can see from Table 4 that in terms of balanced accuracy, OECV performs the best in 12 out of 30 datasets and the 2nd best in 8 data sets. Friedman tests (Demšar, 2006) at the significance level 0.05 reject H0 with the $p$-value $4.21 \times 10^{-3}$, showing that there is a significant difference between methods. The average rank of OECV is 2.167, being the best. Post-hoc tests are then conducted to investigate whether OECV has a significant difference from the competitors, for which OECV is chosen as the control method. Post-hoc comparisons show that OECV can significantly outperform all of the competitors except BEDCOE, where the $p$-value is 0.052, being only marginally higher than 0.05. We conjecture this is because the optimization objective is set to G-mean instead of balanced accuracy in OECV, making the algorithm not aware of this performance metric.

## A.3 Ablation Studies in Terms of Balanced Accuracy

Table 4 shows the predictive performance of the three models in terms of balanced accuracy. Then, the three methods are compared to each other, with Wilcoxon signed rank tests (Wilcoxon, 1992) used to determine if there are significant differences between them.

We can see from Table 4 that in terms of balanced accuracy, the average rank of OECV (1.55) is better than that of OECV-n (2.233) and OECV-ea (2.217). Wilcoxon signed rank test rejects H0 with $p$-value 0.042 and $4.98 \times 10^{-4}$, respectively, meaning OECV is significantly superior to OECV-n and OECV-ea. This indicates that eliminating the EA strategy would significantly decline predictive performance in terms of balanced accuracy, showing its effectiveness.

We follow a similar procedure to compare OECV-ea and OECV-n. In terms of balanced accuracy, the average rank of OECV-ea (2.217) is better than OECV-n (2.233). Wilcoxon signed-rank test fails to reject H0 with

Table 3: Comparison between methods in terms of runtime in seconds. The geometry average of runtime is shown in the last row.

| Dataset | AI-WSELM | MOOB | MUOB | BEDCOE | OECV-n | OECV | OECV-ea |
|---|---|---|---|---|---|---|---|
| Elec | 6.9±1.2 | 49.8±1.4 | 22.5±0.6 | 134.2±3.4 | 6.5±0.1 | 47.5±0.3 | 53.6±3.9 |
| Abrupt | 13.3±2.6 | 51.2±1.5 | 11.2±0.2 | 292.8±20.3 | 6.5±0.3 | 81.4±3.4 | 75.5±1.2 |
| Gradual | 15.0±3.2 | 52.9±0.4 | 5.1±0.1 | 212.8±5.1 | 6.7±0.2 | 110.3±20.5 | 74.9±1.4 |
| Incremental1 | 15.1±3.2 | 49.7±0.2 | 16.2±0.4 | 383.4±5.8 | 6.5±0.2 | 101.5±2.9 | 76.1±1.2 |
| Luxembourg | 5.3±0.1 | 16.4±0.1 | 12.6±0.1 | 28.2±0.5 | 2.5±0.3 | 38.0±2.1 | 27.6±0.7 |
| NOAA | 10.0±0.2 | 48.4±0.2 | 23.8±0.2 | 307.8±13.2 | 7.0±0.7 | 53.9±0.6 | 49.6±0.7 |
| Ozone | 8.0±0.1 | 38.5±1.7 | 6.3±0.3 | 139.4±56.7 | 4.5±0.1 | 55.9±1.8 | 42.7±0.7 |
| Airlines | 12.9±0.4 | 49.0±0.9 | 25.8±0.3 | 364.2±6.4 | 7.3±0.5 | 52.8±0.6 | 47.1±0.4 |
| Covtype | 27.8±0.3 | 58.7±1.0 | 5.3±0.0 | 252.7±4.7 | 7.3±0.2 | 115.4±1.7 | 80.6±1.0 |
| Incremental2 | 17.5±0.5 | 62.4±0.7 | 5.6±0.0 | 379.0±7.1 | 7.2±0.2 | 107.5±3.2 | 75.1±0.9 |
| Abalone1 | 2.4±0.0 | 24.2±0.4 | 4.0±0.2 | 73.4±3.1 | 3.3±0.1 | 25.1±0.4 | 22.7±0.3 |
| Abalone2 | 1.6±0.0 | 16.0±0.4 | 2.5±0.1 | 52.2±1.6 | 2.4±0.2 | 17.4±0.6 | 15.6±0.2 |
| Car1 | 1.6±0.0 | 22.5±0.8 | 4.6±0.8 | 76.5±5.0 | 2.5±0.1 | 18.3±0.3 | 16.4±0.2 |
| Car2 | 1.6±0.0 | 21.3±0.4 | 3.7±0.6 | 46.2±0.7 | 2.5±0.1 | 18.6±0.5 | 16.3±0.1 |
| Kddcup | 7.3±0.3 | 21.1±0.2 | 3.1±0.1 | 36.4±0.8 | 3.3±0.1 | 43.9±2.4 | 31.9±0.6 |
| Kr | 3.8±0.1 | 36.4±0.8 | 5.7±0.4 | 65.9±0.8 | 4.3±0.2 | 30.8±0.6 | 27.4±0.3 |
| Segment | 6.3±0.2 | 31.1±0.6 | 8.9±0.3 | 52.6±1.8 | 3.5±0.4 | 41.4±1.8 | 29.4±0.8 |
| Shuttle1 | 6.4±0.4 | 39.0±1.2 | 6.0±0.5 | 55.4±0.9 | 4.9±0.2 | 38.1±0.5 | 32.5±0.4 |
| Shuttle2 | 3.8±0.2 | 22.9±0.6 | 4.5±0.1 | 31.9±0.8 | 2.8±0.6 | 21.2±0.5 | 17.7±0.2 |
| Thyroid | 2.0±0.1 | 10.1±0.1 | 1.0±0.1 | 37.1±0.6 | 1.2±0.3 | 12.2±0.8 | 8.5±0.3 |
| Win1 | 1.5±0.1 | 7.7±0.2 | 0.9±0.1 | 19.4±0.3 | 1.0±0.2 | 8.4±0.3 | 6.8±0.1 |
| Win2 | 3.6±0.2 | 17.0±0.9 | 3.0±0.2 | 64.6±1.2 | 2.3±0.2 | 18.6±0.5 | 15.5±0.2 |
| Win3 | 1.4±0.1 | 8.1±0.4 | 1.2±0.4 | 23.2±1.1 | 1.0±0.1 | 7.5±0.3 | 6.4±0.1 |
| Win4 | 3.3±0.1 | 16.7±0.4 | 2.2±0.4 | 37.2±1.0 | 2.1±0.1 | 17.0±0.3 | 14.3±0.1 |
| Win5 | 2.0±0.1 | 11.1±0.6 | 1.3±0.1 | 27.7±0.9 | 1.3±0.1 | 10.4±0.3 | 8.7±0.1 |
| Yeast1 | 1.9±0.1 | 13.1±0.8 | 1.7±0.3 | 36.5±0.8 | 1.4±0.1 | 10.2±0.3 | 9.2±0.1 |
| Yeast2 | 3.2±0.1 | 22.5±0.5 | 1.8±0.3 | 150.2±5.2 | 2.1±0.3 | 20.7±0.4 | 15.8±0.1 |
| Yeast3 | 3.1±0.1 | 17.6±0.3 | 4.7±0.2 | 57.5±1.0 | 2.1±0.1 | 15.7±0.2 | 14.5±0.1 |
| Yeast4 | 3.1±0.2 | 17.7±0.5 | 2.4±0.2 | 40.4±0.6 | 2.3±0.6 | 15.6±0.2 | 14.3±0.2 |
| Yeast5 | 3.0±0.1 | 17.4±0.4 | 2.3±0.3 | 42.5±0.7 | 2.1±0.2 | 15.9±0.5 | 14.2±0.1 |
| G-mean time | 4.501 | 24.471 | 4.378 | 75.8 | 3.074 | 28.517 | 23.66 |

$p$-value 0.838, meaning there is no significant difference between OECV-ea and OECV-n. This indicates that using extra samples in the buffer is solely insufficient to find a significantly better cost vector. In other words, although our method uses extra data, this is not the determinative reason why OECV can outperform SOTA methods.

### A.4 Continuous Performance Throughout Time

Figure 5 shows performance comparisons over various time steps on two representative datasets in terms of G-mean and balanced accuracy. Similar patterns were observed in other datasets but are not included here due to space constraints. We can see that OECV consistently outperforms most other methods across most time steps in terms of both G-mean and balanced accuracy. This demonstrates the continuous effectiveness of our approach in improving performance over time.

For ablation studies, we demonstrate continuous performance over time in Figure 6 in terms of G-mean and balanced accuracy. We notice removing the evolutionary cost vector strategy leads to a continual decline in performance across most test steps. As a result, we assert that using EA is crucial in our approach.

Table 4: Performance comparison in terms of balanced accuracy (%). Each entry is the mean±std performance across 10 runs. The best performance on each dataset is highlighted in bold, and the 2nd best performance is highlighted in italics. The last row lists the average ranks (avgRank) of each model across datasets in each subtable. Part (a) reports the comparison between SOTA methods and the proposed OECV. A significant difference against OECV is highlighted in yellow. Part (b) reports the ablation results between variants of OECV.

(a) Performance comparison

| Dataset | AI-WSELM | MOOB | MUOB | BEDCOE | OECV |
|---|---|---|---|---|---|
| Elec | 79.5±1.7 | *91.0±0.2* | 88.9±0.4 | **95.5±0.1** | 84.2±0.9 |
| Abrupt | **68.2±1.1+** | 65.9±0.6 | *67.3±0.6* | 63.7±0.3 | 64.6±0.6 |
| Gradual | 34.1±0.4 | *63.1±0.4* | 20.2±0.8 | **64.1±1.3** | 52.3±1.0 |
| Incremental1 | 48.5±0.6 | **58.6±0.4** | *58.1±0.6* | 54.7±0.4 | 48.2±1.3 |
| Luxembourg | 85.6±2.4 | **100.0±0.0** | **100.0±0.0** | **100.0±0.0** | **100.0±0.0** |
| NOAA | *72.0±0.7* | 66.0±0.6 | 64.9±0.6 | 69.0±0.6 | **73.2±0.5** |
| Ozone | 67.7±2.2 | 74.9±1.3 | **78.3±0.6** | 74.1±1.0 | *77.4±1.6* |
| Airlines | 51.6±0.6 | 51.6±0.5 | 51.1±0.7 | *51.7±0.4* | **52.2±0.8** |
| Covtype | 21.1±2.9 | **70.6±0.4** | 16.4±3.0 | *70.3±0.9* | 38.6±1.1 |
| Incremental2 | 30.1±0.5 | *49.3±0.4* | 25.2±1.9 | **49.4±1.0** | 40.0±0.6 |
| Abalone1 | 60.6±2.3 | 65.6±0.6 | 66.5±2.9 | *68.0±0.5* | **71.9±2.5** |
| Abalone2 | **61.0±3.3** | 51.6±0.2 | 45.2±3.4 | *56.2±0.2* | 54.2±3.1 |
| Car1 | **82.1±2.5** | 53.7±1.1 | 62.4±6.0 | 57.4±2.2 | *79.0±2.1* |
| Car2 | **96.7±2.6** | 77.3±0.5 | 81.2±3.7 | 77.7±1.1 | *96.2±1.0* |
| Kddcup | 83.5±7.3 | **100.0±0.0** | 96.1±3.3 | **100.0±0.0** | **100.0±0.0** |
| Kr | *94.5±1.6* | 94.4±0.7 | 91.0±1.6 | 90.6±0.7 | **94.7±1.2** |
| Segment | 98.7±0.4 | 98.9±0.1 | 93.3±0.6 | *99.0±0.0* | **99.1±0.1** |
| Shuttle1 | **100.0±0.0** | 99.4±0.6 | 98.0±1.7 | 99.1±0.9 | *99.9±0.0* |
| Shuttle2 | 99.4±0.1 | 99.6±0.0 | **99.8±0.1** | *99.7±0.1* | *99.7±0.0* |
| Thyroid | 54.6±4.6 | 53.9±2.8 | 34.7±0.0 | *63.9±1.9* | **75.0±1.5** |
| Win1 | 62.6±14.6 | 53.0±0.1 | 53.4±0.0 | *65.5±15.7* | **83.3±0.5** |
| Win2 | 54.9±1.7 | 51.0±0.9 | **65.0±2.5** | 52.6±0.6 | *64.6±2.0* |
| Win3 | *52.4±2.8* | 51.8±0.8 | 51.5±3.5 | 52.1±1.0 | **80.2±1.2** |
| Win4 | 52.7±1.8 | **59.8±4.6** | 50.1±2.3 | 54.4±0.5 | *59.5±4.4* |
| Win5 | *55.5±5.0* | 53.3±2.0 | 49.4±1.3 | 49.6±0.3 | **58.5±3.8** |
| Yeast1 | **60.1±3.7** | 56.7±0.4 | 53.1±5.8 | 57.1±1.0 | *59.0±7.7* |
| Yeast2 | **45.7±2.7** | 39.4±2.6 | 10.8±1.7 | *41.2±0.8* | 39.9±1.1 |
| Yeast3 | 82.3±2.0 | *89.3±0.3* | **90.1±1.0** | 87.8±0.3 | 87.9±1.0 |
| Yeast4 | 76.7±4.8 | **88.9±0.8** | *84.6±7.4* | 76.7±2.0 | 83.4±4.3 |
| Yeast5 | *75.3±2.4* | 73.5±1.1 | 65.8±4.3 | 66.1±1.9 | **86.8±1.6** |
| avgRank | 3.1 | 3.1 | 3.717 | 2.917 | 2.167 |

(b) Ablation studies

| OECV-n | OECV | OECV-ea |
|---|---|---|
| 83.7±0.4 | **84.2±0.9** | *84.1±0.8* |
| 64.4±0.7 | *64.6±0.6* | **64.7±0.8** |
| **59.2±0.9** | *52.3±1.0* | 50.6±1.1 |
| 47.9±1.1 | **48.2±1.3** | *48.0±1.1* |
| **100.0±0.0** | **100.0±0.0** | **100.0±0.0** |
| *73.1±0.5* | **73.2±0.5** | 73.0±0.5 |
| 73.6±1.4 | **77.4±1.6** | *76.7±1.5* |
| 51.6±0.6 | **52.2±0.8** | **52.2±0.9** |
| **50.1±1.1** | *38.6±1.1* | 33.9±1.2 |
| **43.2±0.6** | *40.0±0.6* | 36.4±0.7 |
| 65.8±1.4 | **71.9±2.5** | *67.2±2.7* |
| 54.0±0.3 | *54.2±3.1* | **54.4±1.8** |
| **79.1±2.4** | *79.0±2.1* | 78.8±1.7 |
| 94.9±1.1 | **96.2±1.0** | *95.3±0.9* |
| **100.0±0.0** | **100.0±0.0** | **100.0±0.0** |
| 91.8±0.7 | **94.7±1.2** | *92.5±1.2* |
| *99.1±0.1* | *99.1±0.1* | **99.4±0.1** |
| **99.9±0.0** | **99.9±0.0** | **99.9±0.0** |
| **99.7±0.0** | **99.7±0.0** | 99.6±0.0 |
| 73.1±2.7 | *75.0±1.5* | **77.1±2.1** |
| *83.5±0.1* | 83.3±0.5 | **83.8±0.6** |
| *60.3±0.4* | **64.6±2.0** | 59.7±1.2 |
| 56.4±2.2 | **80.2±1.2** | *66.0±7.7* |
| *51.2±1.5* | **59.5±4.4** | 51.1±2.2 |
| **63.8±2.7** | *58.5±3.8* | 54.8±4.3 |
| *53.2±0.3* | **59.0±7.7** | 51.6±0.7 |
| **40.0±1.7** | *39.9±1.1* | 36.4±1.7 |
| 85.5±1.0 | **87.9±1.0** | *87.0±0.7* |
| 73.8±3.0 | **83.4±4.3** | *78.5±2.7* |
| *85.7±0.1* | **86.8±1.6** | 83.2±2.2 |
| 2.233 | 1.55 | 2.217 |

### A.5 Analysis on Sensitivity of Population Size

We include a further experiment on the sensitivity of population size setting in OECV. Fixing the other original hyperparameter settings of OECV, we manually alter only the population size (i.e., number of individuals) to get four comparison methods: Pop-25 (original setting), Pop-50, Pop-100, Pop-200, standing for OECV with a population size of 25, 50, 100, and 200, respectively. The detailed comparison setting remains the same as in previous experiments. We report the performance in terms of G-mean in Table 5 and the performance in terms of balanced accuracy in Table 5.

The result shows that increasing the population size wouldn't boost performance significantly, however, the time complexity increases correspondingly. This can be because the problem scale is commonly small in an online learning setting, meaning a small number of individuals can already find a good enough cost vector. We conclude that OECV is not sensitive to this hyperparameter in a certain range. This is also why we only applied a relatively small population size in our main experiment: this setting can significantly improve performance compared to baseline methods while not incurring a long updating delay. In offline learning,

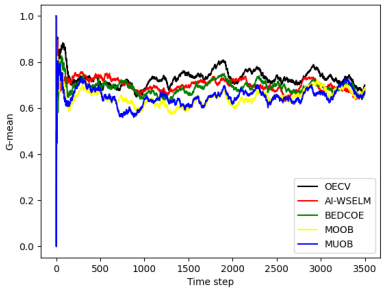


(a) NOAA in G-mean

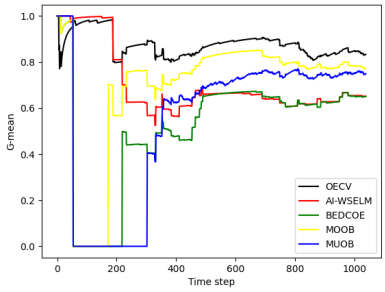


(b) Yeast5 in G-mean

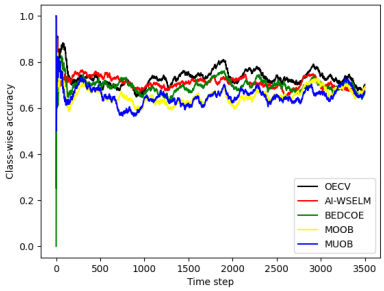


(c) NOAA in class-wise acc.

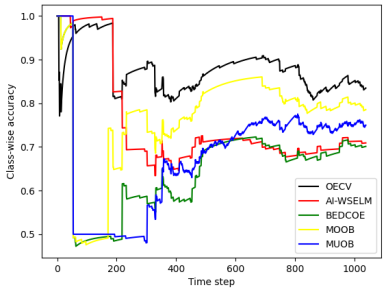


(d) Yeast5 in class-wise acc.

Figure 5: Continuous performance comparison throughout time on representative datasets in terms of G-mean and balanced accuracy.

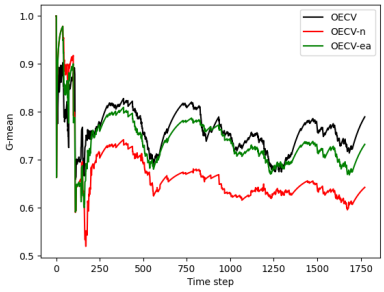


(a) Ozone in G-mean

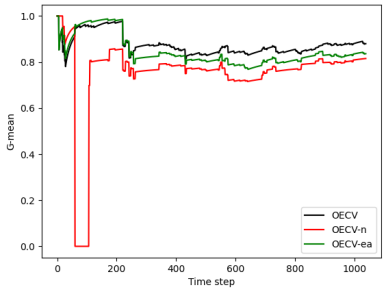


(b) Yeast5 in G-mean

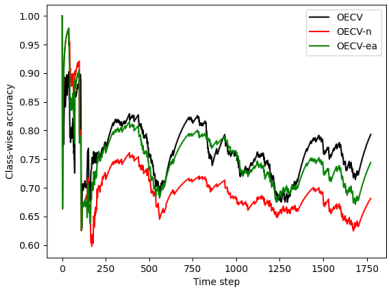


(c) Ozone in class-wise acc.

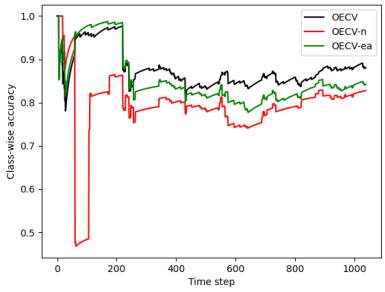


(d) Yeast5 in class-wise acc.

Figure 6: Continuous performance comparison of ablation studies throughout time on representative datasets in terms of G-mean and balanced accuracy.

Table 5: Performance comparison between OECV with different population size in terms of G-mean (%) on the left and balanced accuracy (%) on the right. Each entry is the mean±std performance across 10 runs. The best performance on each dataset is highlighted in bold, and the 2nd best performance is highlighted in italics. The last two rows list the average ranks (avgRank) of each model across datasets, as well as the relative average time costs.

(a) G-mean

| Dataset | Pop-25 | Pop-50 | Pop-100 | Pop-200 |
|---|---|---|---|---|
| Elec | 83.7±7.8 | *83.9±7.8* | 83.8±7.9 | **84.1±7.9** |
| Abrupt | 62.8±3.5 | **63.2±3.5** | *63.1±3.6* | *63.1±3.6* |
| Gradual | 8.5±15.6 | *13.2±19.3* | **24.8±23.6** | 5.5±12.5 |
| Incremental1 | **46.4±5.4** | 46.1±5.7 | 46.2±5.6 | *46.3±5.4* |
| Luxembourg | **100.0±0.0** | **100.0±0.0** | **100.0±0.0** | **100.0±0.0** |
| NOAA | **73.1±4.0** | *73.0±3.9* | 72.9±3.9 | *73.0±4.0* |
| Ozone | 77.1±5.6 | **77.8±5.9** | *77.3±6.0* | 77.0±5.9 |
| Airlines | **51.8±4.7** | 51.7±4.7 | **51.8±4.8** | **51.8±4.7** |
| Covtype | 28.6±15.4 | 36.0±18.4 | *39.0±18.4* | **40.3±18.1** |
| Incremental2 | 15.6±19.5 | 17.2±19.4 | *18.5±17.1* | **20.5±19.3** |
| Abalone1 | *67.8±16.6* | 66.8±16.8 | 67.4±16.7 | **71.9±15.3** |
| Abalone2 | *38.7±24.4* | **51.8±20.2** | 38.2±22.2 | 38.1±20.2 |
| Car1 | *78.2±9.9* | 78.1±9.8 | **78.5±9.9** | 77.6±10.0 |
| Car2 | *96.1±2.0* | **96.2±2.0** | 95.8±1.9 | 95.9±1.7 |
| Kddcup | **100.0±0.0** | 94.9±10.9 | **100.0±0.1** | 98.1±4.5 |
| Kr | *94.7±2.8* | 93.8±3.7 | 93.6±3.7 | **95.1±2.1** |
| Segment | *99.1±0.6* | *99.1±0.6* | **99.2±0.6** | 99.0±0.6 |
| Shuttle1 | **99.9±0.2** | 98.1±6.1 | **99.9±0.2** | 99.8±0.4 |
| Shuttle2 | **99.7±0.6** | 99.6±0.6 | 99.6±0.6 | **99.7±0.6** |
| Thyroid | 71.6±19.2 | 74.4±19.7 | *74.5±19.8* | **76.8±20.3** |
| Win1 | 80.6±18.5 | **84.5±13.8** | 80.3±18.4 | *81.9±15.7* |
| Win2 | 59.2±15.2 | 58.8±12.2 | **61.9±11.3** | *60.1±12.8* |
| Win3 | 79.9±8.2 | **81.5±6.2** | *80.8±6.6* | 80.3±6.6 |
| Win4 | *50.6±20.0* | **64.4±11.9** | 46.6±25.6 | 49.4±25.5 |
| Win5 | 53.3±14.0 | *59.0±9.9* | 57.5±13.3 | **62.8±10.4** |
| Yeast1 | 48.0±29.4 | *51.1±22.6* | 49.2±26.1 | **53.6±22.7** |
| Yeast2 | **0.2±3.0** | *0.1±2.2* | 0.0±0.0 | 0.0±0.9 |
| Yeast3 | **87.8±3.2** | 86.5±3.7 | 86.6±4.0 | *87.2±3.4* |
| Yeast4 | 81.7±13.8 | *86.9±5.6* | 86.5±9.7 | **89.7±4.2** |
| Yeast5 | *86.5±5.8* | **86.6±4.8** | 86.2±5.0 | 85.5±5.0 |
| AvgRank | 2.583 | 2.467 | 2.6 | 2.35 |
| Time cost | ×1 | ×1.11 | ×1.30 | ×1.73 |

(b) Balanced accuracy

| Pop-25 | Pop-50 | Pop-100 | Pop-200 |
|---|---|---|---|
| 83.7±7.8 | *83.9±7.8* | 83.8±7.9 | **84.1±7.9** |
| 62.8±3.5 | **63.2±3.5** | *63.1±3.6* | *63.1±3.6* |
| 8.5±15.6 | *13.2±19.3* | **24.8±23.6** | 5.5±12.5 |
| **46.4±5.4** | 46.1±5.7 | 46.2±5.6 | *46.3±5.4* |
| **100.0±0.0** | **100.0±0.0** | **100.0±0.0** | **100.0±0.0** |
| **73.1±4.0** | *73.0±3.9* | 72.9±3.9 | *73.0±4.0* |
| 77.1±5.6 | **77.8±5.9** | *77.3±6.0* | 77.0±5.9 |
| **51.8±4.7** | 51.7±4.7 | **51.8±4.8** | **51.8±4.7** |
| 28.6±15.4 | 36.0±18.4 | *39.0±18.4* | **40.3±18.1** |
| 15.6±19.5 | 17.2±19.4 | *18.5±17.1* | **20.5±19.3** |
| *67.8±16.6* | 66.8±16.8 | 67.4±16.7 | **71.9±15.3** |
| *38.7±24.4* | **51.8±20.2** | 38.2±22.2 | 38.1±20.2 |
| *78.2±9.9* | 78.1±9.8 | **78.5±9.9** | 77.6±10.0 |
| *96.1±2.0* | **96.2±2.0** | 95.8±1.9 | 95.9±1.7 |
| **100.0±0.0** | 94.9±10.9 | **100.0±0.1** | 98.1±4.5 |
| *94.7±2.8* | 93.8±3.7 | 93.6±3.7 | **95.1±2.1** |
| *99.1±0.6* | *99.1±0.6* | **99.2±0.6** | 99.0±0.6 |
| **99.9±0.2** | 98.1±6.1 | **99.9±0.2** | 99.8±0.4 |
| **99.7±0.6** | 99.6±0.6 | 99.6±0.6 | **99.7±0.6** |
| 71.6±19.2 | 74.4±19.7 | *74.5±19.8* | **76.8±20.3** |
| 80.6±18.5 | **84.5±13.8** | 80.3±18.4 | *81.9±15.7* |
| 59.2±15.2 | 58.8±12.2 | **61.9±11.3** | *60.1±12.8* |
| 79.9±8.2 | **81.5±6.2** | *80.8±6.6* | 80.3±6.6 |
| *50.6±20.0* | **64.4±11.9** | 46.6±25.6 | 49.4±25.5 |
| 53.3±14.0 | *59.0±9.9* | 57.5±13.3 | **62.8±10.4** |
| 48.0±29.4 | *51.1±22.6* | 49.2±26.1 | **53.6±22.7** |
| **0.2±3.0** | *0.1±2.2* | 0.0±0.0 | 0.0±0.9 |
| **87.8±3.2** | 86.5±3.7 | 86.6±4.0 | *87.2±3.4* |
| 81.7±13.8 | *86.9±5.6* | 86.5±9.7 | **89.7±4.2** |
| *86.5±5.8* | **86.6±4.8** | 86.2±5.0 | 85.5±5.0 |
| 2.583 | 2.467 | 2.6 | 2.35 |
| ×1 | ×1.11 | ×1.30 | ×1.73 |

where the problem scale is much larger, especially when the number of classes is larger, a large population size should be applied. We leave the exploration of our method in an offline setting to future work.